Polymer Bulletin (2021) 78:7261–7278
https://doi.org/10.1007/s00289-020-03465-0

ORIGINAL PAPER

Swelling of biodegradable polymers for the production of nanocapsules and films with the incorporation of essential oils

Daniela De Conto[1,2] · Venina dos Santos[2] · Ademir José Zattera[2] · Ruth Marlene Campomanes Santana[1]

Received: 16 March 2020 / Revised: 8 September 2020 / Accepted: 6 November 2020 /
Published online: 19 November 2020

Abstract

Many researchers work with essential oils for several applications, such as their impregnation in polymeric films and for obtaining micro-/nanocapsules by using polymers as shell material. Polymer swelling/liquid dissolution is an extremely important property for controlled release of essential oils. Therefore, this work proposes a comparative study of swelling/dissolution interaction of polymer films immersed in different essential oils. Six polymers were used for this study: polycaprolactone (PCL) and poly(lactic acid) (PLA), gum arabic, sodium alginate, gelatin, and carboxymethyl cellulose. Polymer films were obtained by applying the casting method. In addition, PCL and PLA were molded by compression. Six different essential oils were used: *Mentha piperita, Cymbopogon nardus*, *Mentha arvensis*, *Syzygium aromaticum*, *Lavandula hybrida*, and *Eucalyptus globulus*. Each film was kept at room temperature immersed in sufficient quantity to cover the polymer film at intervals of 1, 3, 5, 7, 14, 28, 56, and 112 days. The same procedure was repeated at 4 °C and 35 °C at intervals of 1, 3, 5, and 7 days. PCL and PLA films were completely dissolved in *Syzygium aromaticum* essential oils for 24 h at the three temperatures tested. For all other polymers, weight gain occurred during the first 7 days and remained constant during the following days. The highest weight gains were 15.519% and 10.463% for polycaprolactone with *Mentha piperita* and gum arabic with *Eucalyptus globulus*, respectively.

Keywords Essential oils · Polymers · Swelling · Encapsulation · Films

✉ Daniela De Conto
daniconto123@gmail.com

[1] Program of Postgraduate Studies in Mining, Metals and Materials Engineering (PPGE3M), Federal University of Rio Grande do Sul (UFRGS), Bento Gonçalves Avenue, 9500, Porto Alegre, Rio Grande do Sul 91501-970, Brazil

[2] Postgraduate Program in Process and Technology Engineering (PGEPROTEC), University of Caxias do Sul (UCS), Francisco Getulio Vargas St., 1130, Caxias do Sul, Rio Grande do Sul 95070-560, Brazil

Introduction

The incorporation of new additives in polymeric materials provides specific properties. Essential oils (EO) are incorporated into biopolymer films to evaluate their antimicrobial efficiency and antibacterial activity among other properties. Studies of Souza et al. [1] developed bionanocomposites based on chitosan/montmorillonite incorporated with two different EO, rosemary (*Rosmarinus officinalis* L.) and ginger (*Zingiber officinale* Rosc), and to evaluate their antimicrobial and antioxidant properties via in vitro assays. Do Evangelho et al. [2] evaluated the morphological, optical, mechanical, and barrier properties and antibacterial activity of corn starch films containing orange EO (*Citrus sinensis*). Corn starch films were prepared by applying the casting method [2]. Tea tree EO was added in different concentrations to starch/furcellaran/gelatin films. The antioxidant properties proved to be significantly enhanced with the addition of EO into films. These films showed antimicrobial activity against *Staphylococcus aureus* and *Escherichia coli*. Results suggested that the films containing EO could be used as an active film which enhances microbial safety and the shelf-life of foods due to its good in vitro antioxidant and antimicrobial properties for food packaging applications [3].

Some paper such as de Flores et al. [4] evaluated the weight gain (swelling) for PCL (by compression), at room temperature (± 23 °C) for 60 days, which had a gain of 9.8% over the initial weight. PLA films obtained by compression molding were evaluated for swelling/solubility in benzyl benzoate and Miglyol 810°R for 13 days. After 48 h at room temperature, complete dissolution of the polymer in benzyl benzoate was observed, while for Miglyol the polymer masses remained unchanged after 13 days, indicating that there was no swelling or dissolution of PLA in this oil [5]. PCL films obtained by compression molding were evaluated for swelling in octyl methoxycinnamate for 13 days ($n = 3$). The experiment showed that polymer weights remained unchanged after 13 days, indicating no swelling or dissolution [6].

EO are volatile organic compounds. They are a mixture of monoterpenes $-C_{10}H_{16}$, two isoprene units, and sesquiterpenes $-C_{15}H_{24}$, three isoprene units and are obtained from aromatic plants. They have been used for thousands of years for producing incenses, food, and medical applications. In addition to its aromatic properties, the EO have numerous properties, such as antimicrobial, antioxidant, antibacterial, antifungal, and anti-inflammatory activities [7–9].

According to Food and Drug Administration (FDA), approximately 160 EO are considered Generally Recognized as Safe (GRAS), which means they can be used safely in food, drugs, and cosmetics. Among them are *Mentha piperita* (MP), *Cymbopogon nardus* (CN), *Mentha arvensis* (MA), *Syzygium aromaticum* (AS), *Lavandula hybrida* (LH) and *Eucalyptus globulus* (EG) [10–12].

Essential oils are also chemically unstable and practically insoluble in aqueous systems. Additionally, EO are susceptible to losses by volatilization and oxidative deterioration when exposed to oxygen, light, heat, or interactions with other matrix ingredients in foods, cosmetics, and pharmaceutical formulations. These disadvantages limit its applications [13, 14].

The encapsulation of EO can solve the problems mentioned above, since the shell isolates EO from external agents, giving them greater stability due to their lower volatility. Furthermore, depending on the chosen encapsulating agent, the release of bioactive compounds is controlled [15–17].

It can be seen remarkable decreases in the amounts of unsaturated terpenes such as γ-terpinene or β-myrcene together with a rise in p-cymene were frequently revealed, especially promoted under light and high temperatures in EO. The storage period and useful life of EO can vary from a few days to years. Also, only a limited number of EO have been subjected to storage experiments [13].

These are some examples of biopolymers (shell materials) used in encapsulation: polysaccharides (gum arabic, modified starches, maltodextrins, alginates, pectin, cellulose derivatives, chitosan, cyclodextrins). Fats and waxes (hydrogenated vegetable oils, lecithin, medium chain triglycerides, glyceryl behenate), proteins (gelatin, whey proteins, sodium caseinate, gluten, caseins, zein), synthetic compounds, or their combinations as polycaprolactone and polylactic acid that are thermoplastics and biodegradables aliphatic polyesters [15, 18]. Furthermore, polymers can act as a versatile wall material to bind or encapsulate a wide variety of bioactive core materials [19].

Studies show that it is possible to determine the amount required to solubilize a single component of the EO by using a variety of techniques, such as UV–visible spectroscopy, fluorescence spectroscopy, and chromatography [20–22]. A method, named total organic carbon, developed to evaluate the solubility of EO inclusion complexes with cyclodextrins [23]. Similarly to Hansen parameters, they give improved agreement with data but are still not completely accurate for predicting the solution thermodynamics for every system [18].

Therefore, a study with more straightforward, efficient, and low-cost techniques is necessary to determine the best shell option to be used in the process, considering that it is not completely dissolved by the EO.

No manuscript provides more detailed information on these interactions, film production method, temperature, and proper direct telling time with statistical tools. The work is relevant to areas related to processes that use polymers in direct contact with EO, or their major components, such as encapsulation processes and films with the incorporation of EO. This is being a simple, inexpensive, and easy to reproduce methodology, thus allowing a prediction of the possibility of use and compatibility of the materials. Since some polymers can be dissolved by essential oils.

The results show that there is no need for prolonged contact periods of polymer films with essential oils, as well as the importance of polymer resistance in direct contact with essential oils.

This work has reported the effect of two methods to obtain polymer films, which were immersed in different EO to provide an understanding on the swelling of these polymers and the importance of the non-dissolution of the shell material (biopolymer) by the material to be encapsulated (essential oil). The chemical potential of the oil in a swollen system is calculated on a macroscopic scale through the mass transfer rate, including the contributions of the swelling (convection-induced diffusion) of the films over time. The results provide information on the swelling/dissolution process over 112 days.

Materials and methods

Materials

Polycaprolactone (PCL) (Mw = 50.000 g mol^{-1}) was obtained from Perstorp, Brazil (commercial name Capa 6500); poly(lactic acid) (PLA) (Mw = 6.800 g mol^{-1}) was obtained from Natureworks®; gum arabic (GA) was obtained from Neon Comércio, Brazil; sodium alginate (SA), gelatine (GE), and carboxymethyl cellulose (CMC) were obtained from Dinâmica Química Contemporânea, Brazil.

The EO of *Mentha piperita* (MP) and *Cymbopogon nardus* (CN) were obtained from Vimontti, Brazil, *Mentha arvensis* (MA), *Syzygium aromaticum* (AS), and *Lavandula hybrida* (LH) from Herbia Cosméticos Orgânicos, Brazil, and *Eucalyptus globulus* (EG) from Arte dos Aromas, Brazil. Acetone (P.A) and chloroform (P.A) were obtained from Química Moderna, Brazil. All reagents were used as received.

Preparation of polymer films

Figure 1 shows the preparation of polymeric films by both methods (casting and compression molding). In the preparation of the films by casting, 2 g of each polymer was dissolved in a volume of 50 mL of its respective solvent, under continuous stirring (Velp Scientifica) until its complete solubilization [24]. Compression

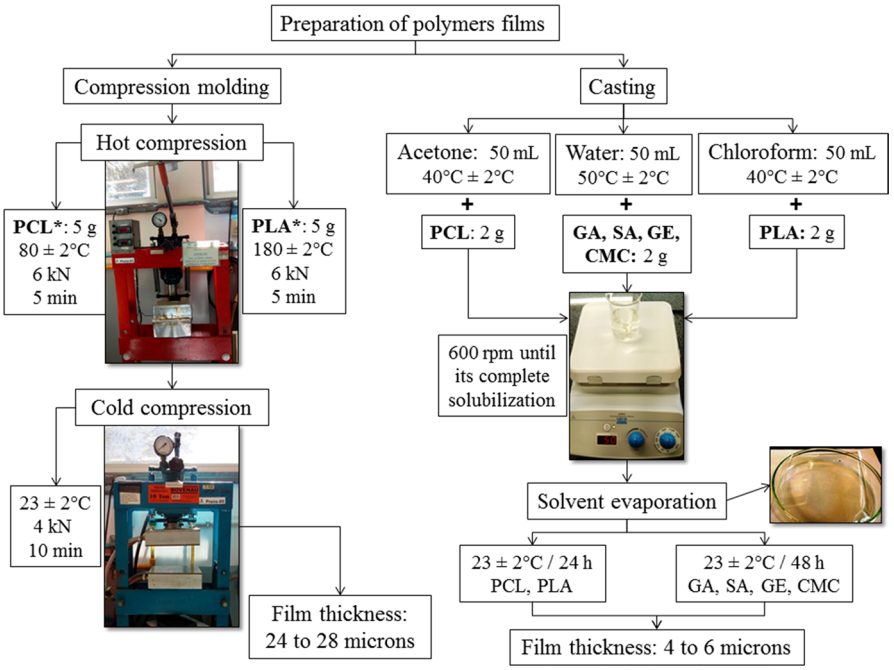

Fig. 1 Preparation of polymeric films

molding (*) was used only for the PCL* and PLA* polymers as described in studies by Guterres et al. [5] and Weiss-Angeli et al. [6]. By using a thermohydraulic press (Bovenau®), the cooling was performed in both, with circulation of water at room temperature. For solvent evaporation in films obtained by casting, all samples were weighed (initial weight = final weight), controlling the absence of solvent traces in the formed films (confirmed by FTIR analysis, Sect. 3.3). The thickness of the films was measured using a manual thickness gauge, model 7301, from the MITUTOYO brand.

Swelling studies

For the study of polymer swelling with EO, 50 mg of each film was placed in contact with each EO. Sufficient quantities of each EO were used to cover the polymer film glass vials in triplicate ($n = 3$). Afterward, the glass vials were closed and kept at room temperature (23 ± 2 °C) for 112 days. At intervals of 1, 3, 5, 7, 14, 28, 56, and 112 days (ensuring a longer contact time of materials), the films were removed from the EO, dried carefully with absorbent paper, and weighed. After weighing, the films were again placed in contact with EO [6, 24]. Due to their structural relationship within the same chemical group, the components of the essential oil are known to easily convert into each other through different reactions. In the process of degradation of EO, the formation of other chemical compounds can occur [13]. So far, the longest period evaluated did not exceed 60 days. To check for the influence of temperature, the same procedure was repeated at 4 °C (refrigerator) and 35 °C (oven) in 7 days. The percentage of weight variation was calculated by using the following empirical relation described in Eq. 1, in which (WD) is the percentage of liquid absorption, (FW) final weight and (SW) starting weight [25, 26]:

$$\mathrm{WD}(\%) = \frac{(\mathrm{FW} - \mathrm{SW})}{\mathrm{SW}} \times 100 \tag{1}$$

Data from the swelling test, in which samples were kept at room temperature for 112 days, were submitted to ANOVA. The F test was used for statistical significance, with alpha equal to 0.05 (95% confidence). Statistical tests that presented statistical significance ($F > F_{\mathrm{critical}}$) were evaluated by multiple comparisons of Duncan's means.

Characterizations

Gas chromatography/mass spectrometry (GC/MS)

GC analyses for all EO were performed on a Hewlett Packard 6890 Series chromatograph equipped with an HP-Chemstation data processor using an HP-Innowax column (30 m × 320 µm id) with 0.50 µm film thickness (Hewlett Packard, Palo Alto, USA). Column temperature was set at 40 °C (8 min), 180 °C at 3 °C min^{-1}, 180–230 °C at 20 °C/min^{-1}, 230 °C (20 min). The injector temperature was set at 250 °C; split ratio at 1:50, flame ionization detector with a temperature of 250 °C;

entrainment gas H_2 (34 kPa). The volume injected was 1µL diluted in hexane (1:10). Analyses were performed on a gas chromatograph coupled to a Hewlett Packard 6890/MSD5973 mass selective detector equipped with HP Chemstation software and Wiley 275 spectrophotometer. A HP-Innowax (30 m × 250 µm) fused silica capillary column 0.50 µm film thickness (Hewlett Packard, Palo Alto, USA). The temperature program used was the same as that used in the GC: interface 280 °C; split ratio 1:100; drag gas He (56 kPa); flow rate: 1.0 mL min^{-1}; ionization energy 70 eV; volume injected 1 µL diluted in hexane (1:10). The constituent oils were identified by comparing their mass spectra with the Wiley library (GC/MS) and by comparing the practical linear retention index with literature data (Nist). The linear retention index was calculated from the Van den Dool and Kratz equation using a standard solution of C_8 to C_{25} hydrocarbons [27].

Field emission scanning electron microscopy (SEM-FEG)

The surface morphology of PCL, PLA, GA, SA, CMC, and GE films prepared by casting and compression-molded PCL* and PLA* was investigated by scanning electron microscopy with a Tescan Mira 3 and Shimadzu SSX-550 Superscan microscope at an acceleration of 10 kV. The samples had previously been sputter coated with gold to increase their electric conductivity.

Fourier transform infrared spectroscopy (FTIR)

The Fourier transform infrared spectroscopy (FTIR-Nicolet IS10-Thermo Scientific) analysis was carried out with 32 scans, within the range of 4000 to 400 cm^{-1}, at a resolution of 4 cm^{-1} by using attenuated total reflectance (ATR) for all polymers as received. The analysis was performed on all polymers after formation the films obtained by both methods and on the films obtained from PCL and PLA by both methods maintained at room temperature for 112 days immersed in MP.

Results and discussion

GC/MS

GC/MS was performed to evaluate the EO components, and the values are shown in Table 1. Several parameters such as ecological condition, harvest time, and extraction techniques can affect the composition of EO [28, 29]. Alcohols, aldehydes, phenylpropanoids, terpenes, and ketones are the main bioactive compounds found in EO and are related to their antioxidant activity [14, 30].

The table shows that the oils with the highest content of one of its components are: *Syzygium aromaticum* (AS) and *Eucalyptus globulus* (EG), 88.09% eugenol, and 83.56% 1.8-cineole, respectively.

Some researchers have found other major components. For instance, EG oil presents eucalyptol (71.51%) and p-cymenene (0.22%) [33], 1,8-cineole (63.6%) and α-terpineol (10.5%) [41], 1,8-cineole 14.55% and α-pinene 1.53% p-cymene 0.49%

Table 1 Major components of EO

EO	Major components	Area (%)	Values from literature (%)	
LH	Linalool	44.95	31.5 [31]	
	Linalyl acetate	24.96	26.8 [31]	
	1,8-Cineole	4.71	7.7 [32, 33]	
AS	Eugenol	88.09	75.41 [34]	88.32–90.22 [35]
	β-Caryophyllene	9.09	0.37 [34]	4.63–6.42 [35]
	α-Caryophyllene	1.56		
MA	I-menthol	47.4	45.49 [36]	56.85 [37]
	Isomenthone	20.89	23.13 [36]	21.13 [37]
	Menthone	10.13	10.42 [36]	
	β-Caryophyllene	5.93	1.32 [36]	
CN	Citronellal	35.18	13.41 [38]	21.8–45.37 [39]
	Geraniol	21.49	11.25 [38]	11.3–20.4 [39]
	Limonene	2.09		
MP	I-menthol	37.94	48.14 [36]	59.73 [37]
	Isomenthone	28.61	0.36 [36]	18.45 [37]
	1,8-Cineole	5.48	5.2 [36]	
	Menthone	4.04	16.78 [36]	
EG	1,8-Cineole	83.56	63.001 [40]	76.66 [29]
	p-cymene	3.87		
	α-Pinene	2.65	16.101 [40]	11.09 [29]

[42], 1,8-cineole 3.16% and α-pinene 0.13% and p-cymene 18.18% [43]. AS oil presents eugenol 81.9%, isoeugenol 13.1% [41], eugenol 57.12–62.88% [44].

Previous studies have also detected menthol and isomenthone as the prevalent constituents in MP [37, 45]. The major component in MP was menthol (45.58%), followed by menthone (24.87%), isomenthone (9.48%), eucalyptol (5.65%), menthyl acetate (4.62%), limonene (2.02%), and β-caryophyllene (1.02%) [46].

SEM-FEG

To verify the surface of the formed films, Fig. 2 shows SEM micrographs of all polymer samples. Films obtained by compression molding had a thickness of 24–28 microns, those obtained by casting with 4–6 microns.

Small particles with different geometric shapes were noted in the GE film. These objects can be undissolved particles (Fig. 2a). The surfaces of the SA and CMC films (Fig. 2c, d) were more homogeneous and smooth. [47–49]. The surface of the GA film (Fig. 2b) showed a weak characteristic and presented cracks in which the oils may have penetrated and been stored, thus increasing their weight gain (Table 2).

The surface of the PCL film (Fig. 2e) exhibited crystals which are large and unequal in size from the nucleation and growth process. Between the crystals it is possible to observe openings in the film, which is one of the signs of the greater

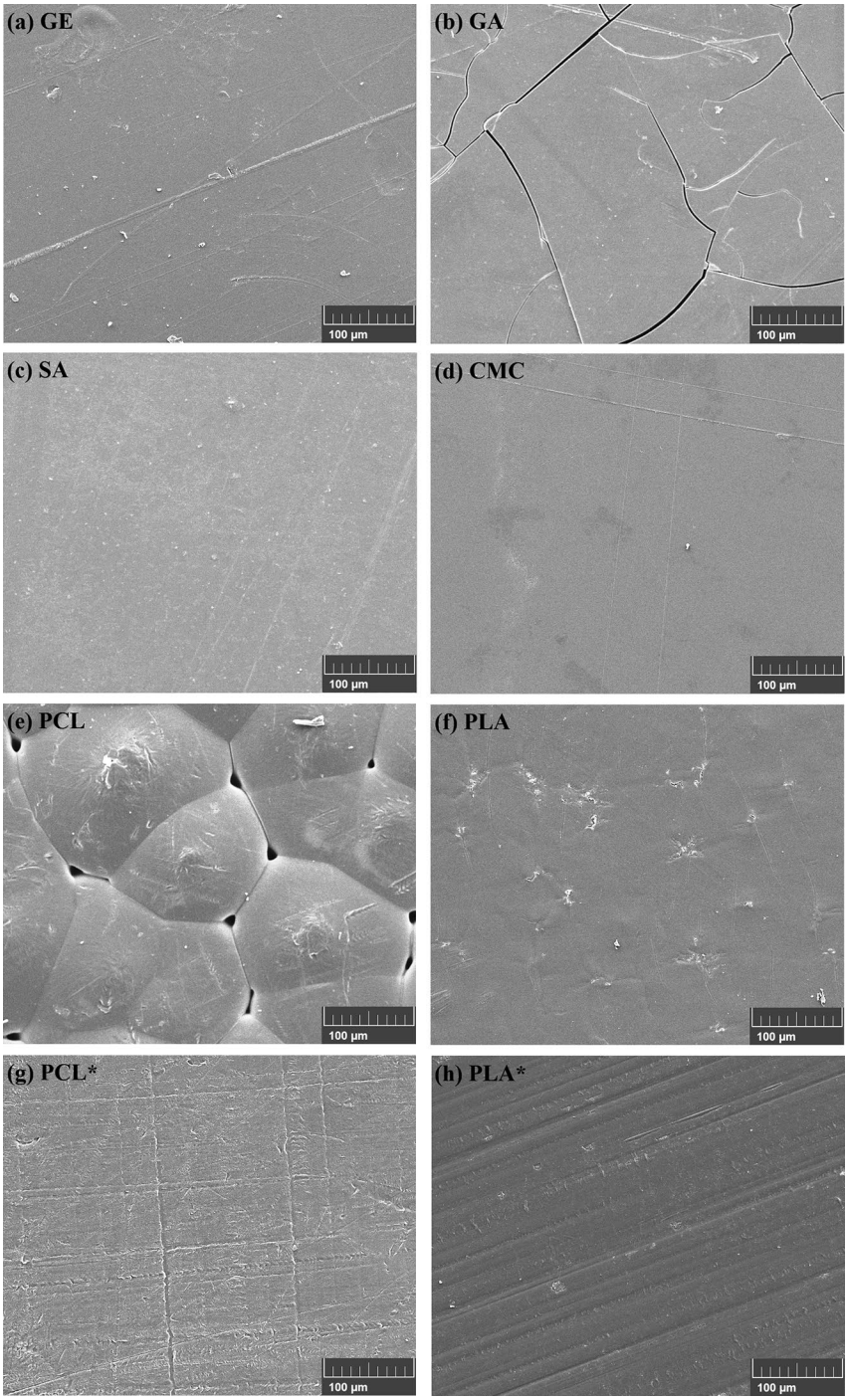

Fig. 2 Surface micrographs of polymer films

Table 2 Weight gain (%) after 112 days immersed in EO

EO	Polymer film							
	PCL	PCL*	PLA	PLA*[D]	GA	GE	CMC[D]	SA
LH[E]	14.224	9.333	0	2.045	9.493	1.208[A]	0	3.690[B]
	±0.426	*±0.291*		*±0.035*	*±0.694*	*±0.748*		*±0.022*
AS	–	–	–	–	8.200[B]	0.793[A]	6.267	3.697[B]
					±0.096	*±0.593*	*±0.173*	*±0.315*
MA[E]	15.29[B]	8.797	0	0.374[A]	8.267[B]	0.628[B]	0	0
	±0.247	±0.018		±0.091	±0.093	±0.012		
CN[E]	15.201[B]	8.181	1.533	2.260[B]	9.495	0.655[A,B,C]	0.821[C]	1.467
	±0.109	*±0.070*	*±0.373*	*±0.015*	*±0.211*	*±0.200*	*±0.187*	*±0.013*
MP	15.519	7.858	0	2.208[B]	9.865	0	1.660	0
	±0.160	*±0.055*		*±0.243*	*±0.035*		*±0.245*	
EG[E]	13.517	6.322	0	1.133	10.463	0.624[C]	0.420[C]	1.847
	±0.243	*±0.011*		*±0.053*	*±0.011*	*±0.042*	*±0.053*	*±0.074*

Italic values indicate average percent absolute error (95% confidence)

([A]) One-way ANOVA—not significant (NS) ratio of initial and final weight

([B]) Two-way ANOVA with repetition (ADR)—NS ratio of polymer to different EO

([C]) ADR—NS ratio of EO to different polymers

([D]) ADR—NS ratio of polymer independent of EO

([E]) ADR—NS ratio of EO independent of polymer

gain for these samples (Table 2) [50]. PLA (Fig. 2f) also presented particles with different geometric shapes on its surface [51].

The micrographs (Fig. 2h) show that the PLA* sample has a grooved surface, probably due to the film preparation process [52, 53]. PCL* (Fig. 2g) presented the same characteristics.

Observing the PLA obtained by compression molding and by casting (Fig. 2f, h) it is noticeable that in both the polymer surface showed irregularities. In comparison with the PCL obtained by both methods (Fig. 2e, g), its surface has a different morphology. Comparing surface images of the PCL film obtained by casting and compression molding, drastic changes in morphology are observed, probably influenced by the cooling time and thinner film formation (4–6 microns). Changes are greater in the casting process (24 h), which favored the growth of crystallites in recrystallization of the PCL, with the formation of spaces between the crystallites. In the case of PLA films, differences are observed. However, they are less intense, but still, small crystallites were observed in the film obtained by casting. This result could indicate that the recrystallization of PLA is much slower than the PCL's [51].

Some polymer films presented a more robust surface, with the formation of cracks or empty spaces, contributing to the weight gain of these films. Figure 3 shows the micrographs of the films with the greatest weight gain, after 112 days of direct contact with EO of MP.

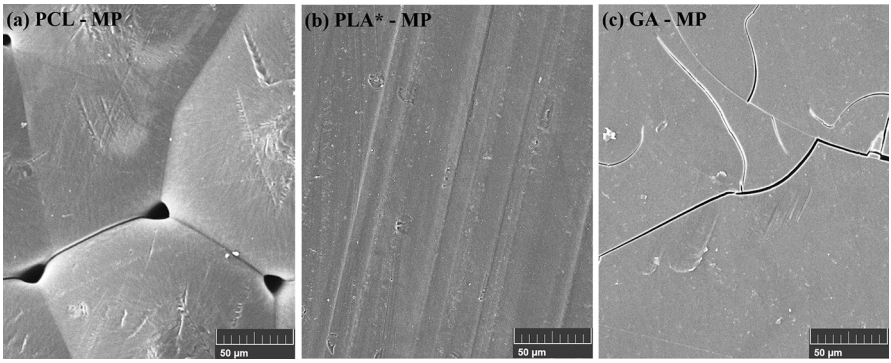

Fig. 3 Surface micrographs of robust polymer films

The surface showed no changes after 112 days in direct contact with EO at room temperature, indicating that the presence of cracks, voids, and undulations can contribute to weight gain, as EO can penetrate and store in these space (Fig. 3).

FTIR

FTIR analysis was applied to identify characteristic absorption bands and is displayed in Fig. 4. This analysis provides important evidence for the reaction because it is sensitive and effective for structural characterization.

Figure 4a shows the IR spectrum of CMC, GA, GE, and SA polymers and their films recorded by the casting method. The characteristic bands remained present for all polymers after film formation, confirming the absence of the solvent. The spectrum of all films exhibits bands of 3668–2998 cm^{-1} attributed to O–H stretching for the hydroxyl group present in all polymers. The CMC band at 2898 cm^{-1} is due to C–H stretching vibration. The presence of a strong absorption band at 1588 cm^{-1} confirms the presence of the COO^- group. The bands around 1416 and 1320 cm^{-1} are assigned to $–CH_2$ scissoring and –OH bending vibration, respectively. The band at 1043 cm^{-1} is due to OCH–O–CH_2 stretching [52, 53], and GA 3321 cm^{-1} O–H stretching, characteristic of glucosidic ring, 1605 cm^{-1} COO– symmetric stretching, 1437 cm^{-1} COO– asymmetric stretching, 1200–900 cm^{-1} finger print of carbohydrates [54]. The absorption bands for gelatin-based composite films containing CO in the IR spectra are situated in the amide band region. The band at 3276 cm^{-1} represents N–H stretching coupled with hydrogen bonding at GE; 1626 (amide I) represents C = O stretching/hydrogen bonding coupled with COO; 1522 (amide II) arises from bending vibration of N–H groups and stretching vibrations of C–N groups; 1240 (amide III) is related to the vibrations in plane of C–N and N–H groups of bound amide or vibrations of CH_2 groups of glycine [47, 55]. The bands at 1592 and 1406 cm^{-1} present in the spectrum of SA are assigned to asymmetric and symmetric stretching bands of carboxylate salt groups. In addition, the bands around 1320 cm^{-1} (C–O stretching), 1130 cm^{-1} (C–C stretching), 1090 cm^{-1} (C–O stretching),

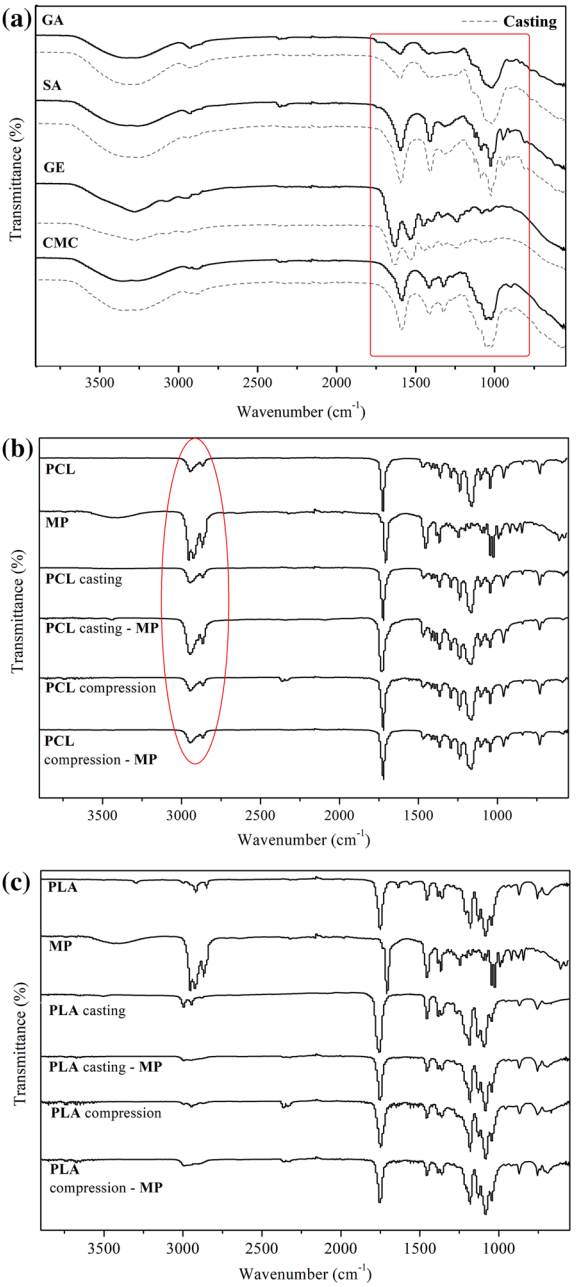

Fig. 4 FTIR of samples: **a** casting polymer films, **b, c** spectra of PCL and PLA films, respectively, and MP essential oil and 112 days after at room temperature

1020 cm^{-1} (C–O–C stretching), and 950 cm^{-1} (C–O stretching) are attributed to its saccharide structure [56, 57].

The spectrum of the MP oil is shown in Fig. 4b, c. The absorption at 3414 cm^{-1} is due to the stretching of hydroxyl groups that are present in the extract (corresponding

to an alcohol group) one of its major compounds 37.94%. The band at 2969 and 2918 cm^{-1} is due to the C–H asymmetric and symmetric stretching of saturated (sp^3) carbon, respectively, 2873 cm^{-1} ascribed to a methyl group. The band at 1695 cm^{-1} is assigned to the bending mode of absorbed water since plant extracts are known to have a strong affinity with water. The band at 1453 cm^{-1} is due to C = C stretching associated with the aromatic skeletal model of the extracts (1027, 1040 cm^{-1}) attributed to the (C–O) bond. The weak bands at 1470 and 968 cm^{-1} are assigned to C–H bending and C–O skeletal vibrations, respectively. The band at 1358 cm^{-1} corresponds to the isopropyl group, all of which confirm the purity of the isolated material [58–60].

The PCL FTIR (Fig. 4b) showed characteristic bands at 2956–2848 (stretching C–H), 1727 (C = O), and 1167–1460 cm^{-1} (deformation CH_2) [61]. As seen earlier (Fig. 2e), the PCL exhibited large and unequal crystals that led to the appearance of voids between these crystals, which must be filled with EO. When ATR FTIR was performed for PCL casting-MP, the reading possibly occurred on a surface that still contained retained EO, thus increasing their weight gain (Table 2).

PLA (Fig. 4c) –CH stretch 2912 cm^{-1} (asymmetric), 2848 cm^{-1} (symmetric), C = O carbonyl stretch 1746 cm^{-1}, $–CH_3$ bend 1447 cm^{-1}, –CH deformation include symmetric and a symmetric band at 1358 cm^{-1}, –C–O– stretch 1179 cm^{-1}, –OH band 1078 cm^{-1}, –C–C– stretch 874 cm^{-1} [62, 63].

Swelling studies

At a storage temperature of 4 °C for 7 days, the polymers showed similar values to those obtained at room temperature for 112 days (Table 2).

PCL and PLA obtained by both methods, immersed in AS oil, had complete dissolution. These results indicate that the AS oil dissolved the polymer forming micellar colloidal dispersions. The complete solubilization of these polymers is associated with their chemical composition that presents more than 88% eugenol, a chemical structure with aromatic ring. PCL and PLA are soluble in benzene [18].

Table 2 presents the percentage values of the acquired weight after 112 days of immersion. The values found for PCL* (by compression) are close to those mentioned by Flores et al. [4], with EO of *Melaleuca alternifolia*, which had a gain of 9.8% over the initial weight.

Two-way ANOVA was performed to compare the averages of the EO. Regardless of the polymer (^{E}), the interaction between LH-CN and MA-EG is NS. Comparing the averages of polymers, independent of the EO (^{D}), the interaction between PLA*-CMC is NS.

By comparing each polymer with the different EO (^{B}), differences were not significant between PCL compared to the MA-CN EO. The same was true for the GE polymer. No significant differences were present when compared to the EO from LH-AS for SA, CN-MP for PLA*, and AS-MA for GA. Comparing each EO with the different polymers (^{C}), no significant differences were noticed among CN samples, compared to the GE-CMC polymers and EG EO for these same polymers.

The PLA-CN presented a final weight gain of only 1.533% ± 0.373. PLA* showed gains which did not exceed 3% in the final weight. The final mass gain (%) for MA is NS. According to Guterres et al. [5], the PLA films obtained by compression molding were evaluated for swelling/solubility in benzyl benzoate and Miglyol 810°R for 13 days. After 48 h at room temperature, complete dissolution of the polymer in benzyl benzoate was observed, while for Miglyol the polymer masses remained unchanged after 13 days, indicating that there was no swelling or dissolution of PLA in this oil [5].

The GE film had a low interaction with all EO, not exceeding 1.3% weight gain by the end of the 112-day period. This low interaction may be related to the crosslinking of polyphenols with proteins (gelatine) under oxidation [64]. Gelatin is insoluble in less polar or nonpolar organic solvents. Amino acids are bound in gelatin by peptide bonds [65].

GA, CMC, and SA are polysaccharides and presented a low interaction with the EO. The highest weight gains are attributed to GA because of its cracked surface structure (Fig. 2b) [66–68]. SA swelling mechanism can be explained by the ionic exchange of monovalent Na^+ ions from the saline solution with the Ca^{2+} ions present in the alginate chain polymanuronate and polyguluronate blocks. For this study, its maximum gain was 3.69% in LH [27]. CMC contains a hydrophobic polysaccharide backbone and many hydrophilic carboxyl groups, which show an amphiphilic characteristic, resulting in its low interaction with EO [52].

Figure 5 shows the weight gain (%) over time for all polymers with different EO over 112 days (1, 3, 5, 7, 14, 28, 56, and 112 days) at room temperature. In some cases the variation of the triplicate is so small, and it is not possible to notice differences in the error bars and does not appear in the graph (Fig. 5).

Some polymers in different EO remained unchanged over time (112 days), such as GE-MP, CMC-LH/MA, SA-MP/MA, and PLA-LH/EG/MP/MA. The other polymers reached balance after 3 days of contact with the EO. According to Weiss-Angeli et al. [6] PCL films obtained by compression molding were evaluated for swelling in octyl methoxycinnamate for 13 days ($n = 3$). The experiment showed that polymer weights remained unchanged after 13 days, indicating no swelling or dissolution.

The sample that was stored at a temperature of 35 °C for 7 days showed values similar to those presented in Table 2. There was complete dissolution for PCL/PCL* in all EO. GA had a decrease in weight of approximately 6% for all EO. This may be related to the softening temperature of the polymers associated with the chemical composition of the EO. As chemical reactions in EO accelerate by increasing heat, van Hoff's law states that a temperature increase of 10 °C approximately doubles the rates of a chemical reaction increases the amount of several unidentified polymerization products formed from myrcene [48, 69].

Also, oil oxidation accelerates with the concentration of dissolved oxygen, which, in turn, depends largely on oxygen partial pressure in the headspace as well as room temperature [70]. Resulting from this conversion (oxidation, isomerization, dehydrogenation reactions, or cyclization, triggered either chemically or enzymatically) they give rise to a range of stable oxidized secondary products

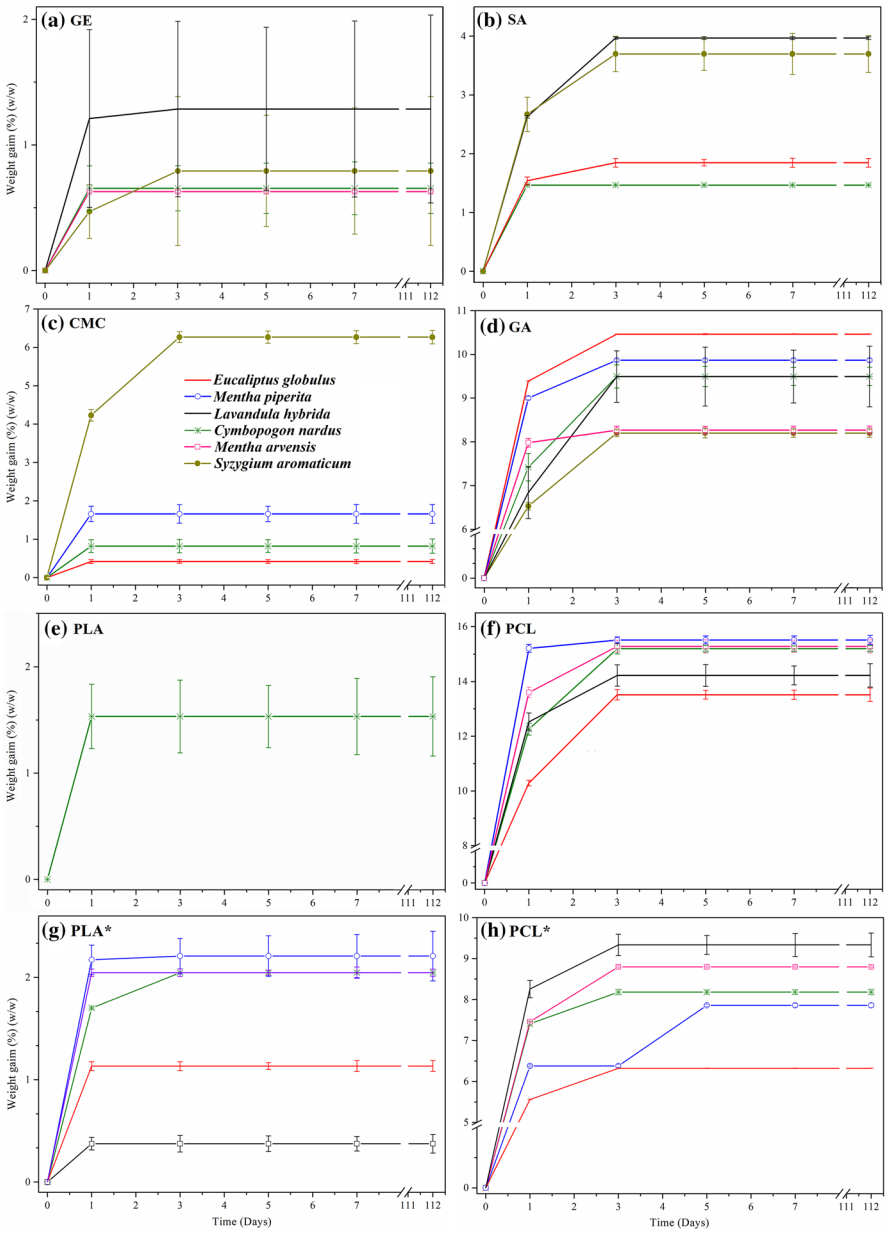

Fig. 5 Weight gain (%) for all polymers with different EO over 112 days at room temperature

such as mono- to polyvalent alcohols, aldehydes, ketones, epoxides, peroxides, or acids as well as highly viscous, often oxygen-bearing polymers [71–73].

These results indicate, except for PCL/PLA-AS, that the other EO and polymers have low macroscopic scale interactions, so much so that the degradation products

of the EO did not interact with the polymers after a long period of contact. Therefore, it is likely that these polymers could serve as wall material in a process of encapsulating EO, which would delay their degradation.

Conclusion

This study identified the need for a prior compatibility test (dissolution/swelling) of polymeric materials to be used as core and shell in encapsulation processes. Depending on the processing method for obtaining polymeric films, their surface morphology may change, which may alter the macroscopic interaction results between the materials involved in a swelling process. The weight gain values at a temperature of 4 °C and 35 °C were similar to room temperature, except for PCL/PCL* completely dissolved for all EO, showing the need to perform this simple process, but temperature conditions in which the material will be exposed. Therefore, this work was limited to comparing 6 polymers, with a weight gain ratio PCL > GA > PCL* > AS > CMC > PLA > GE > PLA*, with 6 EO. Weight gain balance was obtained at 7 days, without the need for longer. It is important to mention that, in general, the results of this study showed that this simple and inexpensive step before processing the production of nano-/microcapsule or films with the incorporation of EO is valuable in ensuring process stability as seen in PCL/PCL* and PLA/PLA*, which completely dissolved in AS within 24 h, for all temperatures. Depending on the temperature and the EO used, all of the polymers studied here have the potential for use in EO encapsulation processes and/or films with the incorporation of EO. PCL and PLA become more advantageous, due to their large-scale production, making their cost less compared to others.

Acknowledgements The authors are grateful for CAPES (Coordination for the Improvement of Higher Education Personnel) and CNPq (Brazilian National Council for Scientific and Technological Development) for the financial support and grants, as well as the laboratories of the University of Caxias do Sul (UCS) and the Federal University of Rio Grande do Sul (UFRGS) for the support in this research.

References

1. Souza VGL, Rodrigues C, Ferreira L, Pires JRA, Duarte MP, Coelhoso I, Fernando AL (2019) In vitro bioactivity of novel chitosan bionanocomposites incorporated with different essential oils. Ind Crops Prod 140:111563
2. do Evangelho JA, da Silva Dannenberg G, Biduski B, el Halal SLM, Kringel DH, Gularte MA, Fiorentini AM, da RosaZavareze E (2019) Antibacterial activity, optical, mechanical, and barrier properties of corn starch films containing orange essential oil. Carbohydr Polym 222:114981
3. Jamróz E, Juszczak L, Kucharek M (2018) Development of starch-furcellaran-gelatin films containing tea tree essential oil. J Appl Polym Sci 135:46754
4. Flores FC, Ribeiro RF, Ourique AF, Rolim CMB, Silva CD, Pohlmann AR, Beck RCR, Guterres SS (2011) Nanostructured systems containing an essential oil: protection against volatilization. Quím Nova 34:968–972
5. Guterres SS, Weiss-Angeli V, Freitas LDL, Pohlmann AR (2000) Influence of benzyl benzoate as oil core on the physicochemical properties of spray-dried powders from polymeric nanocapsules containing indomethacin. Drug Deliv 7:195–199

6. Weiss-Angeli V, Poletto FS, Zancan LR, Baldasso F, Pohlmann AR, Guterres SS (2008) Nanotechnology in the treatment and detection of intraocular cancers. J Biomed Nanotechnol 4:410–418
7. Costa G, Gidaro MC, Vullo D, Supuran CT, Alcaro S (2016) Active components of essential oils as anti-obesity potential drugs investigated by in silico techniques. J Agric Food Chem 64:5295–5300
8. de Cássia da Silveira e Sá R, Andrade L, dos Reis Barreto de Oliveira R, de Sousa D (2014) A review on anti-inflammatory activity of phenylpropanoids found in essential oils. Molecules 19:1459–1480
9. Lee J-H, Lee J, Song KB (2015) Development of a chicken feet protein film containing essential oils. Food Hydrocolloids 46:208–215
10. Prakash B, Kedia A, Mishra PK, Dubey NK (2015) Plant essential oils as food preservatives to control moulds, mycotoxin contamination and oxidative deterioration of agri-food commodities—potentials and challenges. Food Control 47:381–391
11. Rodney Young RT (2014) Essential oil safety, 2nd edn. Churchill Livingstone, London
12. Kfoury M, Auezova L, Greige-Gerges H, Fourmentin S (2019) Encapsulation in cyclodextrins to widen the applications of essential oils. Environ Chem Lett 17:129–143
13. Turek C, Stintzing FC (2013) Stability of essential oils: a review: stability of essential oils. Compr Rev Food Sci Food Saf 12:40–53
14. Burt S (2004) Essential oils: their antibacterial properties and potential applications in foods—a review. Int J Food Microbiol 94:223–253
15. Jafari SM (2017) An overview of nanoencapsulation techniques and their classification. In: Nanoencapsulation Technol. Food Nutraceutical Ind. Elsevier, pp 1–34
16. Akhavan S, Assadpour E, Katouzian I, Jafari SM (2018) Lipid nano scale cargos for the protection and delivery of food bioactive ingredients and nutraceuticals. Trends Food Sci Technol 74:132–146
17. Katouzian I, Faridi Esfanjani A, Jafari SM, Akhavan S (2017) Formulation and application of a new generation of lipid nano-carriers for the food bioactive ingredients. Trends Food Sci Technol 68:14–25
18. Mark JE (ed) (2006) Physical properties of polymers handbook, 2nd edn. Springer, New York
19. Vimala Bharathi SK, Moses JA, Anandharamakrishnan C (2018) Nano and microencapsulation using food grade polymers. In: Gutiérrez TJ (ed) Polymer. Food applications. Springer, Cham, pp 357–400
20. Hill LE, Gomes C, Taylor TM (2013) Characterization of beta-cyclodextrin inclusion complexes containing essential oils (trans-cinnamaldehyde, eugenol, cinnamon bark, and clove bud extracts) for antimicrobial delivery applications. LWT Food Sci Technol 51:86–93
21. Kfoury M, Landy D, Auezova L, Greige-Gerges H, Fourmentin S (2014) Effect of cyclodextrin complexation on phenylpropanoids' solubility and antioxidant activity. Beilstein J Org Chem 10:2322–2331
22. Tao F, Hill LE, Peng Y, Gomes CL (2014) Synthesis and characterization of β-cyclodextrin inclusion complexes of thymol and thyme oil for antimicrobial delivery applications. LWT Food Sci Technol 59:247–255
23. Kfoury M, Lounès-Hadj Sahraoui A, Bourdon N, Laruelle F, Fontaine J, Auezova L, Greige-Gerges H, Fourmentin S (2016) Solubility, photostability and antifungal activity of phenylpropanoids encapsulated in cyclodextrins. Food Chem 196:518–525
24. Santos SS, Lorenzoni A, Ferreira LM, Mattiazzi J, Adams AIH, Denardi LB, Alves SH, Schaffazick SR, Cruz L (2013) Clotrimazole-loaded Eudragit® RS100 nanocapsules: preparation, characterization and in vitro evaluation of antifungal activity against Candida species. Mater Sci Eng C 33:1389–1394
25. Volić M, Pajić-Lijaković I, Djordjević V, Knežević-Jugović Z, Pećinar I, Stevanović-Dajić Z, Veljović Đ, Hadnadjev M, Bugarski B (2018) Alginate/soy protein system for essential oil encapsulation with intestinal delivery. Carbohydr Polym 200:15–24
26. Dadashzadeh A, Imani R, Moghassemi S, Omidfar K, Abolfathi N (2020) Study of hybrid alginate/gelatin hydrogel-incorporated niosomal Aloe vera capable of sustained release of Aloe vera as potential skin wound dressing. Polym Bull 77:387–403
27. dos Santos ACA, Rossato M, Agostini F, Serafini LA, dos Santos PL, Molon R, Dellacassa E, Moyna P (2009) Chemical composition of the essential oils from leaves and fruits of *Schinus molle* L. and *Schinus terebinthifolius* Raddi from Southern Brazil. J Essent Oil Bear Plants 12:16–25
28. Gavahian M, Chu Y-H, Mousavi Khaneghah A, Barba FJ, Misra NN (2018) A critical analysis of the cold plasma induced lipid oxidation in foods. Trends Food Sci Technol 77:32–41

29. Tavakolpour Y, Moosavi-Nasab M, Niakousari M, Haghighi-Manesh S, Hashemi SMB, Mousavi Khaneghah A (2017) Comparison of four extraction methods for essential oil from *Thymus daenensis* subsp *Lancifolius* and chemical analysis of extracted essential oil: four extraction essential oil from *Thymus daenensis* subsp. *Lancifolius*. J Food Process Preserv 41:e13046
30. Nardoni S, Pisseri F, Pistelli L, Najar B, Luini M, Mancianti F (2018) In vitro activity of 30 essential oils against Bovine clinical isolates of prototheca zopfii and prototheca blaschkeae. Vet Sci 5:45
31. Lucia A, Naspi C, Zerba E, Masuh H (2016) Infestation of *Glycaspis brimblecombei* Moore on thirteen *Eucalyptus* species and their relationship with the chemical composition of essential oils. J Insects 2016:1–7
32. Yadav M, Jindal DK, Parle M, Kumar A, Dhingra S (2019) Targeting oxidative stress, acetylcholinesterase, proinflammatory cytokine, dopamine and GABA by eucalyptus oil (Eucalyptus globulus) to alleviate ketamine-induced psychosis in rats. Inflammopharmacology 27:301–311
33. Sharma A, Rajendran S, Srivastava A, Sharma S, Kundu B (2017) Antifungal activities of selected essential oils against *Fusarium oxysporum* f. sp. lycopersici 1322, with emphasis on *Syzygium aromaticum* essential oil. J Biosci Bioeng 123:308–313
34. Gaylor R, Renaud B, Michel J, Panja R, Fanja F, Marc L, Pascal D (2016) Variations in yield and composition of leaf essential oil from *Syzygium aromaticum* at various phases of development. Int J Basic Appl Sci 5:90
35. Štefanidesová K, Špitalská E, Csicsay F, Friedländerová V, Šáner A, Škultéty Ľ (2019) Evaluation of the possible use of genus Mentha derived essential oils in the prevention of SENLAT syndrome caused by Rickettsia slovaca. J Ethnopharmacol 232:55–61
36. de Sousa Guedes JP, da Costa Medeiros JA, de Souza e Silva RS, de Sousa JMB, da Conceição ML, de Souza EL (2016) The efficacy of *Mentha arvensis* L. and *M. piperita* L. essential oils in reducing pathogenic bacteria and maintaining quality characteristics in cashew, guava, mango, and pineapple juices. Int J Food Microbiol 238:183–192
37. Clain E, Baranauskienė R, Kraujalis P, Šipailienė A, Maždžierienė R, Kazernavičiūtė R, El Kalamouni C, Venskutonis PR (2018) Biorefining of *Cymbopogon nardus* from Reunion Island into essential oil and antioxidant fractions by conventional and high pressure extraction methods. Ind Crops Prod 126:158–167
38. Ríos N, Stashenko EE, Duque JE (2017) Evaluation of the insecticidal activity of essential oils and their mixtures against *Aedes aegypti* (Diptera: Culicidae). Rev Bras Entomol 61:307–311
39. Mekonnen A, Yitayew B, Tesema A, Taddese S (2016) *in vitro* antimicrobial activity of essential oil of *Thymus schimperi*, *Matricaria chamomilla*, *Eucalyptus globulus*, and *Rosmarinus officinalis*. Int J Microbiol 2016:1–8
40. Orchard A, Kamatou G, Viljoen AM, Patel N, Mawela P, van Vuuren SF (2019) The influence of carrier oils on the antimicrobial activity and cytotoxicity of essential oils. Evid Based Complement Alternat Med 2019:1–24
41. Mulyaningsih S, Sporer F, Zimmermann S, Reichling J, Wink M (2010) Synergistic properties of the terpenoids aromadendrene and 1,8-cineole from the essential oil of E*ucalyptus globulus* against antibiotic-susceptible and antibiotic-resistant pathogens. Phytomedicine 17:1061–1066
42. Hafsa J, Smach MA, Ben Khedher MR, Charfeddine B, Limem K, Majdoub H, Rouatbi S (2016) Physical, antioxidant and antimicrobial properties of chitosan films containing *Eucalyptus globulus* essential oil. LWT Food Sci Technol 68:356–364
43. de Oliveira MS, da Costa WA, Pereira DS, Botelho JRS, de Alencar Menezes TO, de Aguiar Andrade EH, da Silva SHM, da Silva Sousa Filho AP, de Carvalho RN (2016) Chemical composition and phytotoxic activity of clove (*Syzygium aromaticum*) essential oil obtained with supercritical CO_2. J Supercrit Fluids 118:185–193
44. Almeida ET da C, de Souza GT, de Sousa Guedes JP, Barbosa IM, de Sousa CP, Castellano LRC, Magnani M, de Souza EL (2019) *Mentha piperita* L. essential oil inactivates spoilage yeasts in fruit juices through the perturbation of different physiological functions in yeast cells. Food Microbiol 82:20–29
45. Al-Daraghmeh MY, Hayajneh MT, Almomani MA (2019) Corrosion resistance of TiO_2–ZrO_2 nanocomposite thin films spin coated on AISI 304 stainless steel in wt% NaCl solution. Mater Res 22:e20190014
46. Chuysinuan P, Chimnoi N, Reuk-Ngam N, Khlaychan P, Makarasen A, Wetprasit N, Dechtrirat D, Supaphol P, Techasakul S (2019) Development of gelatin hydrogel pads incorporated with Eupatorium adenophorum essential oil as antibacterial wound dressing. Polym Bull 76:701–724
47. Łupina K, Kowalczyk D, Zięba E, Kazimierczak W, Mężyńska M, Basiura-Cembala M, Wiącek AE (2019) Edible films made from blends of gelatin and polysaccharide-based emulsifiers—a comparative study. Food Hydrocolloids 96:555–567

48. Fox K, Tran PA, Lau DWM, Ohshima T, Greentree AD, Gibson BC (2016) Nanodiamond-polycaprolactone composite: a new material for tissue engineering with sub-dermal imaging capabilities. Mater Lett 185:185–188
49. Sharma D, Satapathy BK (2019) Mechanical Properties of Aliphatic Polyester-Based Structurally Engineered Composite Patches. Macromol Symp 384:1800153
50. Savaris M, dos Santos V, Brandalise RN (2016) Influence of different sterilization processes on the properties of commercial poly(lactic acid). Mater Sci Eng, C 69:661–667
51. Patra S, Mohanta KL, Parida C (2019) Mechanical properties of bio-fiber composites reinforced with *luffa cylindrica* irradiated by electron beam. Int J Mod Phys B 33:1950305
52. Rani M, Rudhziah S, Ahmad A, Mohamed N (2014) Biopolymer electrolyte based on derivatives of cellulose from kenaf bast fiber. Polymers 6:2371–2385
53. Pushpamalar V, Langford SJ, Ahmad M, Lim YY (2006) Optimization of reaction conditions for preparing carboxymethyl cellulose from sago waste. Carbohydr Polym 64:312–318
54. Appolonia Ibekwe C, Modupe Oyatogun G, Ayodeji Esan T, Michael Oluwasegun K (2017) Synthesis and characterization of chitosan/gum arabic nanoparticles for bone regeneration. Am J Mater Sci Eng 5:28–36
55. Nur Hanani Z, Beatty E, Roos Y, Morris M, Kerry J (2013) Development and characterization of biodegradable composite films based on gelatin derived from beef, pork and fish sources. Foods 2:1–17
56. Smitha B, Sridhar S, Khan AA (2005) Chitosan–sodium alginate polyion complexes as fuel cell membranes. Eur Polym J 41:1859–1866
57. Moreira APD, Sader MS, de Soares GD A, Leão MHMR (2014) Strontium incorporation on microspheres of alginate/β-tricalcium phosphate as delivery matrices. Mater Res 17:967–973
58. Mathur A, Prasad GB, Rao N, Babu P, Dua VK (2011) Isolation and identification of antimicribial compound from *Mentha pipirita*. Rasayan J. 4:36–42
59. Pramila DM (2012) Phytochemical analysis and antimicrobial potential of methanolic leaf extract of peppermint (*Mentha piperita:* lamiaceae). J Med Plants Res. https://doi.org/10.5897/JMPR11.1232
60. Ferreira CC, de Sousa LL, Ricci VP, da Rigo EC S, Ramos AS, Campos MGN, Mariano NA (2019) Titanium biomimetically coated with hydroxyapatite, silver nitrate and polycaprolactone, for use in biomaterials (biomedicine). Mater Res 22:e20190177
61. Shoja M, Shameli K, Ahmad MB, Kalantari K (2015) Preparation, characterization and antibacterial properties of polycaprolactone/Zno microcomposites. Dig J Nanomater Biostruct 10:169–178
62. Kister G, Cassanas G, Vert M (1998) Effects of morphology, conformation and configuration on the IR and Raman spectra of various poly(lactic acid)s. Polymer 39:267–273
63. Ai X, Wang D, Li X, Pan H, Kong J, Yang H, Zhang H, Dong L (2019) The properties of chemical cross-linked poly(lactic acid) by bis(tert-butyl dioxy isopropyl) benzene. Polym Bull 76:575–594
64. Strauss G, Gibson SM (2004) Plant phenolics as cross-linkers of gelatin gels and gelatin-based coacervates for use as food ingredients. Food Hydrocolloids 18:81–89
65. Domb AJ, Kost J, Wiseman D (1998) Handbook of biodegradable polymers, 1st edn. Taylor & Francis Ltd, London
66. Mariod AA (2018) Functional properties of gum arabic. In: Gum Arab. Elsevier, pp 283–295
67. Masuelli MA (2013) Hydrodynamic properties of whole arabic gum. Am J Food Sci Technol 1:60–66
68. Anderson DMW, Douglas DMB, Morrison NA, Weiping W (1990) Specifications for gum arabic (*Acacia Senegal);* analytical data for samples collected between 1904 and 1989. Food Addit Contam 7:303–321
69. Santos PS Reimpressão 2002 sob a supervisão de. 354
70. Choe E, Min DB (2006) Mechanisms and factors for edible oil oxidation. Compr Rev Food Sci Food Saf 5:169–186
71. Bäcktorp C, Hagvall L, Börje A, Karlberg A-T, Norrby P-O, Nyman G (2008) Mechanism of air oxidation of the fragrance terpene geraniol. J Chem Theory Comput 4:101–106
72. Bluman A 2040 Blumann and Ryder : Autoxidation of u-Phellandrene. 436. Autoxidation of a-Phellandrene 4
73. Karlberg A-T, Shao LP, Nilsson U, Gäfvert E, Nilsson JLG (1994) Hydroperoxides in oxidized d-limonene identified as potent contact allergens. Arch Dermatol Res 286:97–103